Received: 2 April 2019 | Revised: 6 November 2019 | Accepted: 7 November 2019

DOI: 10.1002/cne.24819

RESEARCH ARTICLE

JCN RESEARCH IN SYSTEMS NEUROSCIENCE THE JOURNAL OF COMPARATIVE NEUROLOGY WILEY

Exosome/microvesicle content is altered in leucine-rich repeat kinase 2 mutant induced pluripotent stem cell-derived neural cells

Kate M. Candelario[1] | Leonora Balaj[2] | Tong Zheng[3] | Johan Skog[4] | Bjorn Scheffler[5] | Xandra Breakefield[2] | Birgitt Schüle[6] | Dennis A. Steindler[1,3]

[1]Department of Neurological Surgery, McKnight Brain Institute, University of Florida, Gainesville, Florida

[2]Massachusetts General Hospital and Harvard University, Boston, Massachusetts

[3]JM USDA Human Nutrition Research Center on Aging, and CTSI of Tufts University, Boston, Massachusetts

[4]Exosome Diagnostics, Inc., Cambridge, Massachusetts

[5]DKFZ-Division of Translational Oncology/ Neurooncology, German Cancer Consortium (DKTK), Heidelberg & University Hospital Essen, Essen, Germany

[6]Department of Pathology, Stanford University, Stanford, California

Correspondence
Dennis A. Steindler, PhD
Email: stemcellguy@gmail.com

Funding information
Michael J. Fox Foundation for Parkinson's Research, Grant/Award Number: N/A; U.S. Department of Agriculture, Grant/Award Number: USDA/ARS grant 1950-51000-081-00D.; University of Florida; USDA; Michael J. Fox Foundation

Abstract

Extracellular vesicles, including exosomes/microvesicles (EMVs), have been described as sensitive biomarkers that represent disease states and response to therapies. In light of recent reports of disease-mirroring EMV molecular signatures, the present study profiled two EMVs from different Parkinson's disease (PD) tissue sources: (a) neural progenitor cells derived from an endogenous adult stem/progenitor cell, called adult human neural progenitor (AHNP) cells, that we found to be pathological when isolated from postmortem PD patients' substantia nigra; and (b) leucine-rich repeat kinase 2 (LRRK2) gene identified patient induced pluripotent stem cells (iPSCs), which were used to isolate EMVs and begin to characterize their cargoes. Initial characterization of EMVs derived from idiopathic patients (AHNPs) and mutant LRRK2 patients showed differences between both phenotypes and when compared with a sibling control in EMV size and release based on Nanosight analysis. Furthermore, molecular profiling disclosed that neurodegenerative-related gene pathways altered in PD can be reversed using gene-editing approaches. In fact, the EMV cargo genes exhibited normal expression patterns after gene editing. This study shows that EMVs have the potential to serve as sensitive biomarkers of disease state in both idiopathic and gene-identified PD patients and that following gene-editing, EMVs reflect a corrected state. This is relevant for both prodromal and symptomatic patient populations where potential responses to therapies can be monitored via non-invasive liquid biopsies and EMV characterizations.

KEYWORDS

extracellular vesicles RRID 000067128, Parkinson's disease RRID 010300, stem cells RRID 13234

1 | INTRODUCTION

Parkinson's disease (PD), the second most common neurodegenerative disease and the most common degenerative movement disorder, has seen advances in understanding the etiology, disease course, and treatment from studies in the stem cell biology and regenerative medicine field (for review, see Steindler, Okun, & Scheffler (2012)). In particular, cell culture, transgenic rodent models, and xenograft studies have become a gold standard for studying genetic, molecular, cellular, and systems biology for translation to the clinic where applying regenerative medicine holds hope for neuroprotection and repair in PD. Conventional diagnosis and treatment of neurodegenerative

disease consists of neurological evaluation, brain imaging, and, most recently, genomic screening with a list of at-risk mutations.

Histopathologically, PD is characterized by the presence of alpha-synuclein (α-syn), a cytosolic protein involved in synaptic vesicle function and neurotransmitter release (Burre et al., 2010; Nemani et al., 2010). α-syn protein aggregates contribute to a proteinopathy that is associated with at-risk neurons first in the brainstem, including the vagal complex and dopaminergic neurons of the substantia nigra pars compacta, and then spreading rostral to forebrain structures in so-called Braak's stages that have been argued to potentially correlate with disease progression and behavioral losses (Braak & Del Tredici, 2009; Burke, Dauer, & Vonsattel, 2008). Analysis of transplanted fetal midbrain dopamine neurons in PD patients has shown that these cells can acquire and potentially spread the α-syn proteinopathy, possibly via an infectious cell-to-cell transmission manner (Kordower, Chu, Hauser, Freeman, & Olanow, 2008). The role of infectious agents, including pathogens such as the H5N1 bird flu virus (Jang et al., 2009), involved in the potential etiology of PD also includes recent observations from our lab of *toxoplasma gondii* infection. This type of infection affects over one third of all humans and was shown to modulate signature pathways of PD, other neurodegenerative diseases, and cancer (Ngo et al., 2017). Clinically, PD is a movement disorder most typified by tremor at rest, slow, and altered movements, and a variety of non-motor symptoms. These symptoms include altered sleep behavior associated with REM sleep disorder as well as autonomic changes, and cognitive decline that is most associated with late stage disease (Braak & Del Tredici, 2009; Pfeiffer, 2012). Mutations in the gene leucine-rich repeat kinase 2 (LRRK2) leads to gene programming of a protein involved in inflammatory and other tissue/somatic functions including oxidative phosphorylation and mitochondrial dynamics (Sanders et al., 2014). These mutations cause late onset PD in 1–8% of both autosomal dominant disease transmitting families as well as sporadic disease (Fraser et al., 2013) that most often leads to a diagnosis usually by exclusion. Ninety percent of PD cases are idiopathic (non-inherited), with the remainder harboring such a known genetic mutation that is correlated with PD phenotype and behavior (Cookson & Bandmann, 2010).

In the present study, we investigate induced pluripotent stem cell (iPSC)-derived neural cells from gene identified, patient skin-punch derived fibroblasts with a LRRK2 G2019S mutation, and compare them with controls (patient non-PD sibling) as well as gene-corrected cells (Sanders et al., 2014). The utilization of iPSCs facilitates personalized, precision medicine because it affords studying a patient's unique neural cell genetic makeup. In line with previous studies that have reported the generation of phenotype-expressing neurodegenerative disease at-risk neurons and glia, the induced pluripotency cellular reprogramming approach bypasses decades to manifest disease in patients (Israel et al., 2012). In PD, several studies have now confirmed the presence of exosomes/microvesicles (EMVs) with cargoes that contain both LRRK2 and α-syn in cultured cells, in animals, and in human biofluids (Fraser et al., 2013; Fraser, Moehle, Alcalay, West, & Consortium, 2016; Fraser, Rawlins, et al., 2016; Stuendl et al., 2016). The current study aimed to compare EMVs released from iPSC-derived neural cells with those from adult human neural progenitor (AHNP) cells that we have previously characterized from normal adult human brain as well as from idiopathic PD autopsy specimens (Walton et al., 2006; Wang et al., 2012).

The study of EMVs has wide therapeutic potential such that they can be detected in accessible fluids including CSF, urine, and blood (Cai, Janku, Zhan, & Fan, 2015). Although we are not certain as to all of the different types of microvesicles that might be released from the at-risk cells under the conditions studied here, the term EMVs is used here synonymously with exosomes (Tomlinson et al., 2015). The use of EMVs as a diagnostic tool holds promise for earlier detection of PD and contributes to precision medicine that lead to treatment options directed at PD rather than misdiagnosis of another movement or neurodegenerative disorder. Understanding the similarities of neural cells derived from PD patient's iPSCs are comparable to brain-derived neural cells, which may help with future therapeutic treatments for their disease. EMVs, shed from cell membranes, range from 30–1,000 nm in size. Exploration of exosomes and other extracellular vesicles have been performed in various cell types, including cells of the central nervous system, which have been shown to be able to carry DNA, RNA (including miRNAs), and/or protein (Candelario & Steindler, 2014). Given the attention EMVs have received recently for their biomarkers and disease prognostic potential, their distinct phenotype, and their potential to play a therapeutic role (Candelario & Steindler, 2014; Rajendran et al., 2014, for review) efforts have been made to study the role of EMVs in the characterization of disease status and propagation of PD (Alvarez-Erviti et al., 2011; Fraser et al., 2013; Gui, Liu, Zhang, Lv, & Hu, 2015; Loov, Scherzer, Hyman, Breakefield, & Ingelsson, 2016; Tomlinson et al., 2015). Even though neural cells including astrocytes, neurons, and microglia have been well-documented to release EMVs under and/or contributing to different cellular states including lysosomal status, ER stress, and neuroinflammation (Brockmann et al., 2016; Eitan, Suire, Zhang, & Mattson, 2016; Fernandes et al., 2016; Gupta & Pulliam, 2014), the present study began as a proof-of-principle to show that: (a) we can employ methods for isolation of EMVs from iPSCs/neural progenitor cells (NPCs) and small sample volumes; (b) identify EMV-release from NPCs and dopaminergic neurons; and (c) Identify alterations in exosome cargo related to mutations in LRRK2.

Our studies show that EMVs are shed from iPSC-derived neural cells that have a G2019S mutation in the LRRK2 gene. We found that EMVs with the G2019S LRRK2 mutation have alterations in gene expression compared with control EMVs. Furthermore, gene expression from cargo analysis of EMVs derived from LRRK2 iPSC-derived dopamine neuron precursors can be normalized to control (non-PD sibling) following gene correction of these cells. These results have the potential to contribute to the identification of new biomarkers for PD.

2 | MATERIAL AND METHODS

The use of human cells for this study was approved by the University of Florida Institutional Review Board. The animal studies performed here were approved by the Institutional Animal Care and Use Committee of the University of Florida (Approval #: 201507304).

2.1 | Cell culture

AHNPs were isolated from postmortem tissue samples or electrodes used for deep brain stimulation as previously described (Walton et al., 2006). PD-AHNPs studied here were isolated from the substantia nigra of a patient with PD. Control AHNPs were isolated from the hippocampus of a patient with epilepsy to serve as a non-Parkinsonian, non-neurodegenerative control. AHNPs were expanded on poly-ornithine-coated 6 cm dishes and cultured in growth medium (Walton et al., 2006; Wang et al., 2012) containing bFGF (20 ng/ml), LIF (10 ng/ml), and 5% exosome-depleted fetal calf serum (dFCS).

To deplete FCS of exosomes (dFCS), 20% FCS in growth medium is ultracentrifuged for 16 hr at 100,000*g* at 4°C. When cells are 70% confluent, the cells are washed and media containing 5% dFCS is added to the cultures. Cells are incubated in media with dFCS for 48 hr to condition the media with EMVs, and cell debris is removed (Thery, Amigorena, Raposo, & Clayton, 2006).

iPSCs: iPSCs were generated from a patient that harbored a point mutation in the *LRRK2* gene, known as NM_198578.3 (LRRK2): c.6055G>A (p.Gly2019Ser) (abbreviated in this article as LRRK2 G2019S; cell line PI-1.13), as well as from a healthy sibling (control; cell line PI-1815). For a more detailed description of individual iPSC clones, see Supplemental Table 1 in Sanders et al. (2014). The LRRK2 G2019S iPSC line was edited using zinc-finger nuclease-driven targeted gene editing to create an iPSC line that was corrected for the mutation (cell line PI-1.7). Control (PI-1815), LRRK2 G2019S heterozygote (PI-1.13), and LRRK2 G/S correction (1.7; zinc-finger nuclease-[ZFN]-driven targeted gene editing, Urnov et al., 2005) were described previously (Sanders et al., 2014) for ZFN-mediated genomic repair of LRRK2 G2019S in iPSCs. A population/convenience control iPSC line was also obtained from the Coriell Institute for Medical Research (ND41865). For iPSCs requiring a feeder layer, mouse embryonic fibroblasts (MEFs) from CF-1 mice that had been inactivated with mitomycin C (MTI-Global Stem, Gaithersburg, MD) were cultured on tissue culture-treated plates in DMEM containing Glutamax (2 mM; Invitrogen), FCS (15%), and penicillin–streptomycin (100 units/ml; Invitrogen). MEFs were cultured overnight or for up to 5 days prior to coculture with iPSCs. For coculture with iPSCs, MEFs were washed with phosphate buffered saline (PBS), and iPSCs were plated as colonies in DMEM/F12 without glutamine (Invitrogen), Knockout Serum Replacement (20%; Invitrogen), Glutamax (1 mM; Invitrogen), non-essential amino acids (NEAA; 0.1 mM; Sigma Aldrich), beta-mercaptoethanol (βME; 55 μM), penicillin–streptomycin (100 units/ml; Invitrogen), heparin (2 μg/ml), and basic fibroblast growth factor (bFGF; 6 ng/ml). Rock inhibitor Y27632 (10 μM; Sigma) was used with thawing or passaging of iPSCs. After two passages following thawing, iPSCs were transferred to feeder-free conditions on Matrigel (Corning) in mTesr1 media (Stemcell Technologies) supplemented with penicillin–streptomycin (100 units/ml; Invitrogen). iPSCs were passaged as colonies using dispase (10 μg/ml; Stemcell Technologies).

To differentiate iPSCs, embryoid body (EB) formation was performed using Aggrewell 800 plates and following the manufacturer's instructions (Stemcell Technologies). Briefly, iPSCs were dissociated with Accutase (Sigma) for 10 min at 37°C. Dissociated iPSCs were plated at a concentration of 1.2×10^6 cells per well. Formation of EBs was performed in culture media containing 10 μM ROCK inhibitor, DMEM/F12, KOSR (20%), NEAA (0.1 mM), penicillin–streptomycin (100 units/ml; Invitrogen), βME (0.1 mM), Glutamax (0.5×), Dorsomorphin (5 μM; Sigma), and SB431542 (10 μM; Tocris) (Mak et al., 2012; Xi et al., 2012).

After 24 hr in the Aggrewell, EBs were harvested using a reversible 37 μm strainer and plated in low binding plates at a concentration at less than 1,000 EBs per well of a six-well plate in EB formation media. The media was changed every 2 days, and 4 days later the EBs were harvested and transferred to polyornithine- and laminin-coated plates. Cells were then cultured in neural induction media (NIM) containing DMEM/F12, 1× NEAA, 0.5× L-glutamine, bFGF (20 ng/ml), heparin (2 μg/ml), and penicillin–streptomycin (100 units/ml; Invitrogen), along with the N2 supplement containing rh-insulin (5 μg/ml), h-Transferrin (100 μg/ml), NaSel (sodium selenite) (30 nM), progesterone (20 nM), and putrescine (100 μM). The media was changed every 2 days until the appearance of neural rosettes (approximately 12 days in vitro). To isolate neural rosettes, the wells were washed with DMEM/F12 and incubated in dispase (10 μg/ml) for 5 min. The dispase was removed and the well was washed with DMEM/F12. Neural rosettes were scraped using a cell lifter and triturated using a P200 pipette tip. These human iPS-derived neural progenitor cells (hiNPCs) were resuspended in NPC culture media containing Neurobasal media, Pen/strep, 1× B27, 1× NEAA, bFGF, heparin, and Glutamax. Cells were grown on tissue culture plates coated with Geltrex (ThermoFisher Scientific), and passaged 1:2 until the desired number of cells were obtained.

For subsequent differentiation into dopaminergic neurons, iPS-derived NPCs were cultured in neurobasal media containing Glutamax (2 mM, Invitrogen), 1× NEAA (Sigma), 1× B27 (Invitrogen), SHH (200 ng/ml, R&D Systems), and FGF8 (100 ng/ml, R&D Systems). On Day 11, medium was changed to Neurobasal media containing Glutamax (2 mM, Invitrogen), 1× NEAA, 1X B27, BDNF (20 ng/ml, R&D Systems), GDNF (20 ng/ml, R&D Systems), and cAMP (1 mM, Sigma) for 14 days (Mak et al., 2012; Xi et al., 2012). For differentiation into astrocytes, NPCs were cultured in 5% FCS for 10 days. For differentiation into oligodendrocytes, NPCs were cultured in 0.5% FCS with 1 ng/ml PDGFA for 21 days (Zhang, Ge, & Duncan, 2000).

2.2 | Immunocytochemistry

Cells that were to be examined by immunocytochemistry were cultured on glass coverslips that were coated with poly-L-ornithine (15 μM; Sigma Aldrich) followed by laminin (10 μg/ml; Invitrogen) (Goetz et al., 2006). Cultured cells were fixed on coverslips with 4% paraformaldehyde in PBS. Cells were permeabolized and blocked with PBS supplemented with 10% FCS, 5% normal goat serum, and 0.1% Triton X-100, and incubated in the primary antibodies against nestin,

tyrosine hydroxylase (TH), β-III tubulin (Tuj1), Lmx1a, NeuN, Sox1, Vimentin, GFAP, CNPase, and myelin basic protein (MBP) (for details, see Table 1). Immunofluorescence was visualized using fluorescent-labeled secondary antibodies (1:500, Invitrogen). DAPI nuclear stain (1 μg/ml; Invitrogen) was used to identify cell bodies. The coverslips were mounted onto a slide using Vectashield Mounting Medium for Fluorescence (Vector Laboratories, Inc., Burlingame, CA) and examined using a fluorescence microscope.

2.3 | Animals

Immunodeficient mice, NOD.Cg-Prkdc^{scid} Il2rg^{tm1Wjl}/SzJ (NSG, The Jackson Laboratory, Stock# 005557), were used as recipients for iPSC-derived neural progenitor cell transplantations. All adult breeding pairs were maintained in a climate-controlled environment and exposed to a 12 hr light/dark cycle daily. They were housed one pair per cage, and offered water and diet ad libitum. The day pups were born was considered as day 0, and the transplantation procedures were performed at 0–3 days post-delivery (P0-3).

2.4 | Cellular transduction with green fluorescent protein

The control human iPS cells used for our xenograft studies were purchased from the Coriell Institute for Medical Research (ND41865). They were differentiated into neural progenitor cells as described earlier. These hiNPCs were labeled with green fluorescent protein (GFP) before transplanted into animals. Low passage cells at 30–50% confluency were transduced with replication incompetent GFP-Lenti viral vectors as we have previously described (Walton et al., 2006) (the vector is a gift from Dr. Lung-Ji Chang, University of Florida Department of Molecular Genetics and Microbiology). For transduction, hiNPCs were pre-treated with 5 μg/mL hexadimethrine bromide and incubated with 1–5 MOI of virus for 24 hr. GFP+ human cells were

TABLE 1 Primary antibodies used in this study

Antibody	Immunogen	Source	RRID, type, raised in	Working dilution
Anti-nestin	Fusion protein corresponding to human Nestin clone 10C2	EMD Millipore Cat# MAB5326	AB_2251134, Monoclonal, mouse	1:200
Anti-tyrosine hydroxylase	Denatured tyrosine hydroxylase from rat pheochromocytoma	EMD Millipore Cat # AB152	AB_390204, Polyclonal, rabbit	1:250
Anti-Tuj1	Synthetic peptides corresponded to human and rat β-Tubulin 3 gene	Aves Labs Inc., Cat# TUJ	AB_2313564, Polyclonal, chicken	1:500
Anti-GFP	Purified recombinant green fluorescent protein (GFP)	Aves Labs, Cat# GFP-1020	AB_10000240, Polyclonal, chicken	1:1000
Anti-human nuclear antigen	Nuclei of human myeloid leukemia biopsy cells	Millipore, Cat# MAB1281	AB_94090, Monoclonal, mouse	1:500
Anti-Doublecortin	Synthetic peptide corresponding to Human Doublecortin aa 350	Abcam Cat# 77450	AB_2088478, Polyclonal, rabbit	1:1000
Anti-zona occludens-1	A 69 kD fusion protein corresponding to amino acids 463–1,109 of human ZO-1 cDNA.	Invitrogen, Cat # 61–7,300	AB_2533938, Polyclonal, rabbit	1:100
Anti-Lmx1a	Synthetic peptide within Human LMX1A aa 300–350 (C terminal)	Abcam, Cat# ab139726	AB_2316106, Polyclonal rabbit	1:50
Anti-NeuN	Purified cell nuclei from mouse brain	EMD Millipore, Cat# MAB377	AB_2298772, monoclonal mouse	1:100
Anti-Sox1	KLH-conjugated linear peptide corresponding to human SOX1 near the N-terminus	EMD Millipore, Cat#AB5934	AB_92124, polyclonal chicken	1:300
Anti-Vimentin	Synthetic peptide within human vimentin aa 400 to the C-terminus (C terminal) (acetyl)	Abcam Cat # ab92547	AB_2216258, monoclonal rabbit	1:200
Anti-GFAP	GFAP isolated from cow spinal cord	Dako, Cat# Z0334	AB_10013382, polyclonal rabbit	1:100
Anti-CNPase	Purified human brain CNPase	EMD Millipore, Cat # MAB326	AB_2082608, monoclonal mouse	1:100
Anti-Myelin basic protein	Human myelin basic protein from brain	EMD Millipore, Catalog # AB980	AB_92396, polyclonal rabbit	1:200

Note: Supporting Information is provided which shows qPCR data of all genes studied here, relevant to neurodegenerative disease and stem cells, and PD-related and corrected genes as shown in Figure 5.

sorted on a FACSDiva (BD, Franklin Lakes, NJ) to obtain a pure GFP+ cell populations two passages after transduction. Purified GFP+ cells were then expanded for several passages before transplantation.

2.5 | Transplantation

All transplant procedures and anesthetics were performed or administered at University of Florida and were in accordance with University of Florida and NIH regulations governing the ethical care and handling of laboratory animals. Selected GFP+ donor cells were collected and transplanted into the striata or cortex of NSG newborn mice. Mouse pups (P0–P3) were cryo-anesthetized and stably immobilized. Illumination light was used to help identify landmarks such as sutures and sinuses through the scalp for visual guidance. 1.0 μL of cells (50,000–100,000/μL) were injected into the target area during each injection and two injections were made in adjacent areas in each pup. Pups were cleaned and kept warm and then returned to their dam. They were closely monitored until fully recovered and tended to by their mothers.

2.6 | Tissue processing and immunohistochemistry

Following various survival times, mice were deeply anesthetized with isofluorane, and transcardially perfused with 4% paraformaldehyde in 0.1 M PBS (pH = 7). Mouse brains were cryostat sectioned in parasagittal planes at a thickness of 30 μm. To examine the degree of survival and differentiation of the grafted cells, the cells were identified by their expression of GFP, human nuclear antigen and doublecortin (DCX, Table 1). Immunofluorescence was visualized using fluorescent-labeled secondary antibodies (1:500; Invitrogen). Sections were evaluated using an epifluorescence microscope and an Olympus IX81-DSU Spinning Disk confocal microscope.

2.7 | Nanosight vesicle number and size

To measure EMV number and size, conditioned media were collected and analyzed using Nanosight instrumentation in combination with Nanoparticle Tracking Analysis (Malvern Panalytical, Malvern, United Kingdom). Cell culture supernatant was collected and centrifuged at 300*g* for 5 min, followed by centrifugation at 2000*g* for 15 min at 4°C. Supernatant was then passed through a 0.8 μm filter prior to use or freezing the supernatant at -80°C. EMV number and size were analyzed.

2.8 | EMV gene expression

RNA isolation from EMVs was performed from conditioned culture media, processed as described earlier for Nanosight, using the exoRNeasy kit according to manufacturer's recommendation (QIAGEN and ExosomeDx). The TaqMan® OpenArray® Human Stem Cell Plate was used to characterize gene expression markers specific to human stem cell-related genes (ThermoFisher Scientific). OpenArrays were run in duplicates, and the correlation between runs had correlation coefficients over 0.96. To determine the Log2-fold change and compare gene expression between EMVs shed from each cell line, the average C_{rt} value of the control genes was subtracted from the C_{rt} values for each target gene. If a C_{rt} value for a gene was not determined in the array, that gene was not analyzed. Log2-fold change values were calculated using Microsoft Excel. GraphPad Prism was used to generate both a heat map and a graph of the data.

3 | RESULTS

3.1 | iPSCs differentiate into neurons via a neural progenitor cell intermediate in vitro and in vivo

In order to study a known mutation responsible for a majority of inherited PD cases, we utilized iPSCs that were reprogrammed from patient skin fibroblasts with the LRRK2 G2019S mutation as well as from control patients (either population control or sibling of the PD patient). To generate a population of dopaminergic neurons in vitro, iPSCs were differentiated toward a neural lineage through the use of growth factors known to result in ventral midbrain patterning. iPSCs were differentiated into neural progenitor cells via EB formation followed by subsequent neural rosette formation (Figure 1). NPCs isolated from neural rosettes were expanded (Figure 1d). These NPCs maintain the ability to self-renew and proliferate in culture over several passages.

By definition, stem and progenitor cells are capable of self-renewal as well as possess the potential to become a more differentiated subtype. Here, we show NPCs differentiated from a control iPSC line were immunopositive for SOX1, nestin, and the ventral midbrain marker Lmx1A (Figure 2a–c). To determine whether the NPCs we differentiated from iPSCs were multipotent, NPCs were terminally differentiated into neurons, astrocytes, and oligodendrocytes. Culturing of NPCs first with SHH and FGF8 followed by culture with BDNF, GDNF, and cAMP lead to differentiation into dopaminergic neurons as analyzed by their expression of neuronal markers TH, β-III Tubulin, and NeuN (Figure 2d–f). Differentiation of NPCs into astrocytes in the presence of fetal calf serum (5%) produced vimentin- and GFAP-positive cells (Figure 2g,h). Differentiation of NPCs into oligodendrocytes by culturing NPCs in the presence of fetal calf serum (0.5%) and PDGFA (1 ng/ml) resulted in oligodendrocytes that were immunopositive for MBP and CNPase (Figure 2i,j). These data indicate that the iPSC-derived NPCs we generated are multipotent and are capable of terminal differentiation into mature dopaminergic neurons.

To confirm that the iPSC-derived NPCs are also capable of differentiating into neurons in vivo, GFP-labeled hiNPCs were

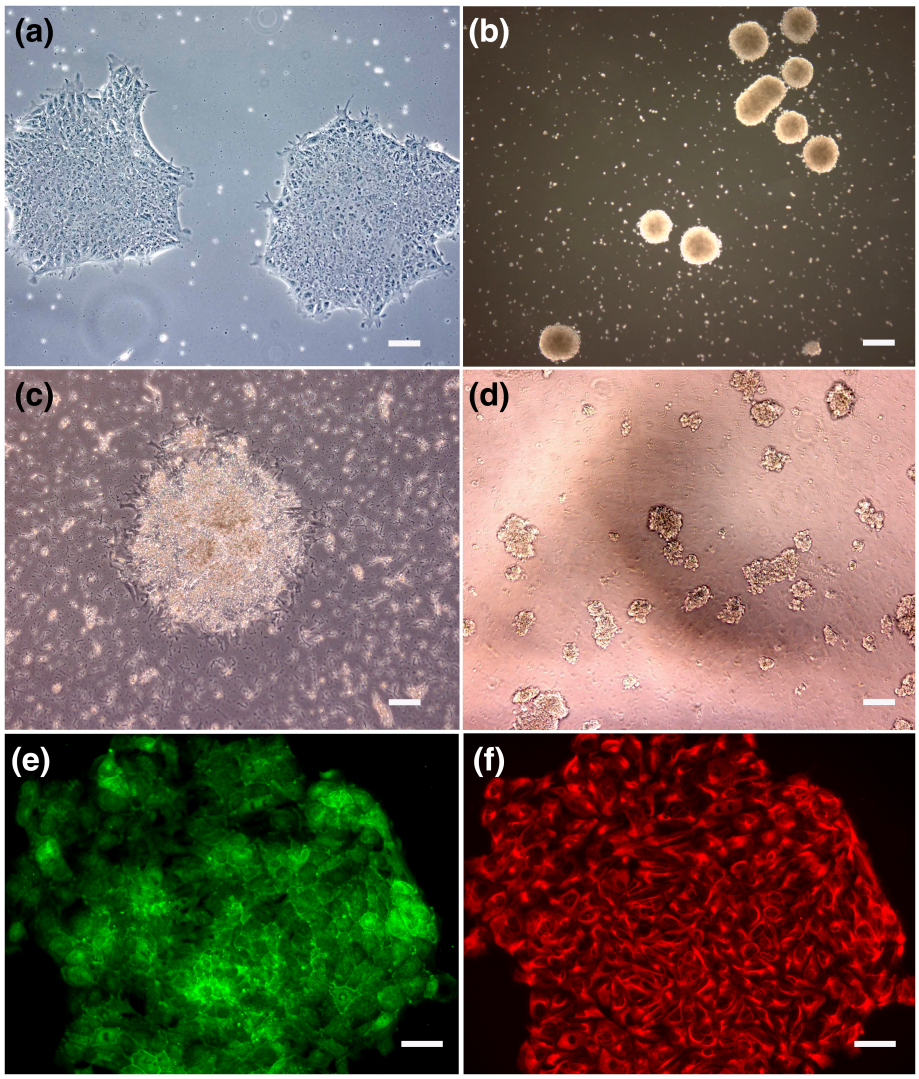

FIGURE 1 iPSC differentiation into neural progenitor cells. Representative images under phase contrast microscopy of the different stages of iPSC differentiation including iPSC colonies (a), embryoid bodies (b), neural rosette (c), and neural progenitor cells (d). Immunostaining of a neural rosette for the markers nestin (e) and ZO-1 (f). Scale bars for images a, c, and d (10×) = 20 μm, for image b (4×) = 50 μm, and images e and f (20×) = 10 μm [Color figure can be viewed at wileyonlinelibrary.com]

transplanted into mouse neonate brains, the donor cells were found to survive and differentiate into neurons that were immunopositive for DCX (Figure 2m). GFP-positive donor cells, also identified by human specific nuclear antigen (Figure 2l), survived for up to 6 months post-transplant and extended neurites throughout the injection sites.

3.2 | Neural cells from Parkinson's disease patients shed EMVs

One way to detect and measure pathology is to evaluate the content of extracellular vesicles, which are released from cells, circulate throughout the body, and are present in a variety of patient biofluids, including CSF, blood, and urine. Extracellular vesicles, including exosomes, have been shown to be shed from a variety of cell types including those of neural origin (Rajendran et al., 2014) under both physiological and pathological conditions; the latter of which is presumed to be associated with disease state or response to therapeutic regimens.

We chose to first analyze EMVs from brain-derived AHNPs cells because of our prior study of normal and PD primary lines with cells that were initially isolated from deep brain stimulation electrodes or postmortem tissue samples from idiopathic disease (Wang et al., 2012). We used AHNPs from a patient with epilepsy to serve as a non-PD, non-neurodegenerative control. Conditioned media from cultured AHNPs were analyzed using Nanosight instrumentation in combination with Nanoparticle Tracking Analysis software to measure the number and size of secreted microvesicles (Figure 3a). In addition, vesicle number and size were analyzed from conditioned media from iPSC-derived neural progenitor cells (Figure 3b) and iPSC-derived dopaminergic neurons (Figure 3c). For iPS cells, control, LRRK2 mutant, and zinc-finger G/S gene corrected lines were analyzed. Vesicles from control AHNP cells have a mean size of 180 nm and 3.89×10^8 particles/ml, whereas vesicles from PD-AHNP cells have a mean size of 151 nm and 4.59×10^8 particles/ml (Figure 3a). Control iPSC-derived neural progenitor cells have a mean vesicle size of 132.6 nm and a concentration of 7.08×10^8 particles/ml, LRRK2 mutant iPSC-derived neural progenitor cells have a mean vesicle size of 161.8 nm and a

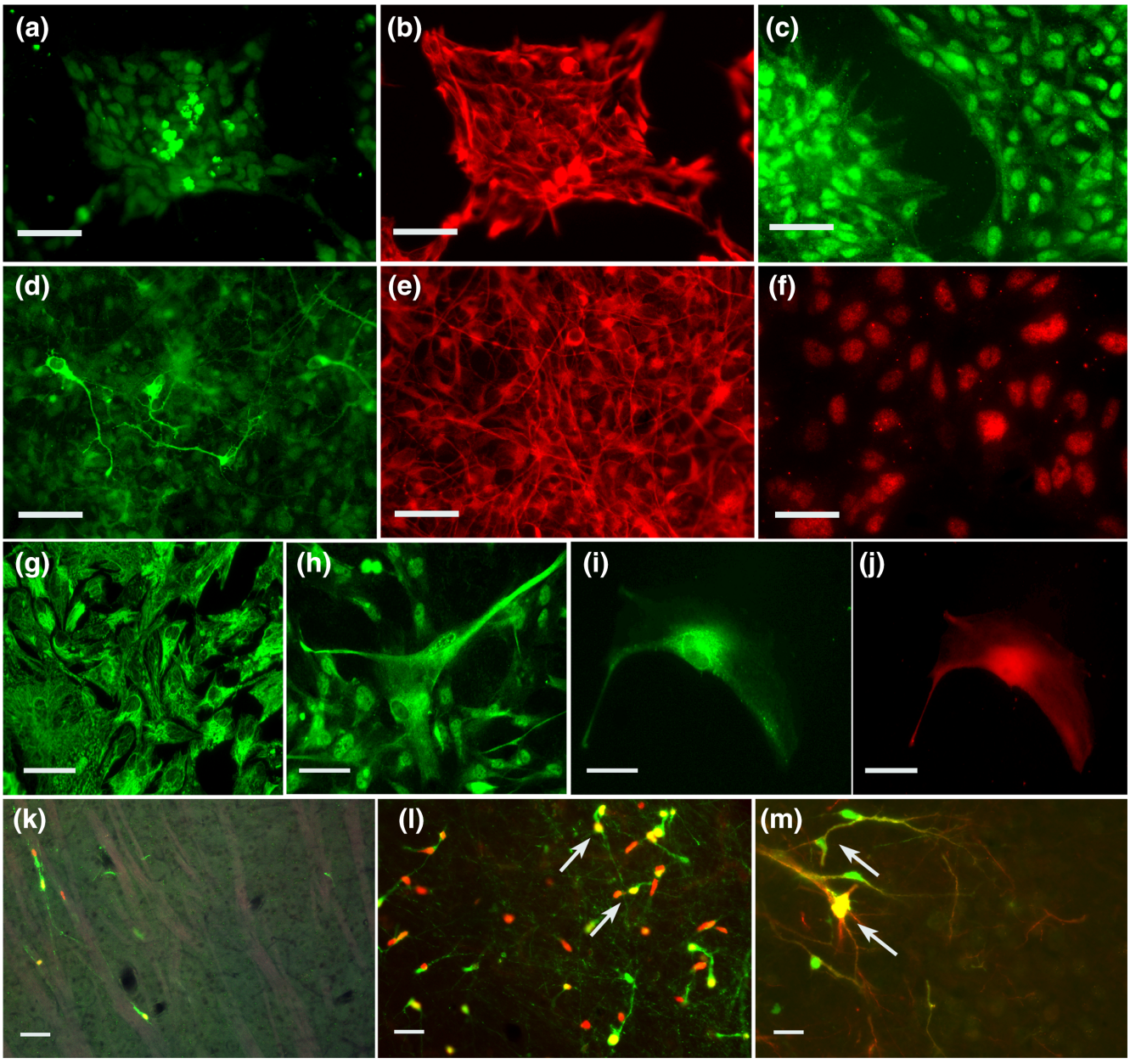

FIGURE 2 iPSC-derived neural progenitor cell differentiation in vitro and in vivo. iPSCs were differentiated into multipotent neural progenitor cells that express the stem cell markers SOX1 (a) and nestin (b), as well as the ventral midbrain marker Lmx1a (c). iPSC-derived neural progenitor cells are multipotent such that differentiation leads to the phenotypic expression of markers for neurons (d–f), astrocytes (g, h), and oligodendrocytes (i, j). iPSC-derived neurons expressed tyrosine hydroxylase (TH) + (d), the intermediate filament protein Tuj1 (e), and the neuronal nuclei marker NeuN (f). Differentiation of iPSC-derived neural progenitors into astrocytes yields vimentin-positive (g) and GFAP-positive (h) cells. Differentiation of iPSC-derived neural progenitors into oligodendrocytes yields CNPase-positive (i) and MBP-positive (j) cells. Transplantation of hiPSC-derived neural progenitor cells transfected with GFP into newborn mouse striatum appeared to integrate into the striatum of the host brain (k). Immunofluorescent images of brain sections show GFP+ NSCs (green) present in the striatum 70 days post-transplantation (k). Transplanted GFP+ cells are positive for the neuronal migration marker doublecortin (DCX, m) and express human nuclear antigen (HNA) (l). Arrows pointed to double labeled cells (yellow) in l & m. scale bar = 50 μm in a–c, and 10 μm in d–f [Color figure can be viewed at wileyonlinelibrary.com]

concentration of 2×10^8 particles/ml, and corrected iPSC-derived neural progenitor cells have a mean vesicle size of 179.3 nm and a concentration of 2.8×10^8 particles/ml (Figure 3b). Control iPSC-derived dopaminergic neurons have a mean vesicle size of 185.8 nm and a concentration of 3.03×10^8 particles/ml, LRRK2 mutant iPSC-derived dopaminergic neurons have a mean vesicle size of 234.5 nm and a concentration of 4.83×10^8 particles/ml, and corrected iPSC-derived dopaminergic neurons have a mean vesicle size of 198.6 nm and a concentration of 2.43×10^8 particles/ml (Figure 3c). Figure 4 shows how the G2019S mutation in the LRRK2 gene alters the most

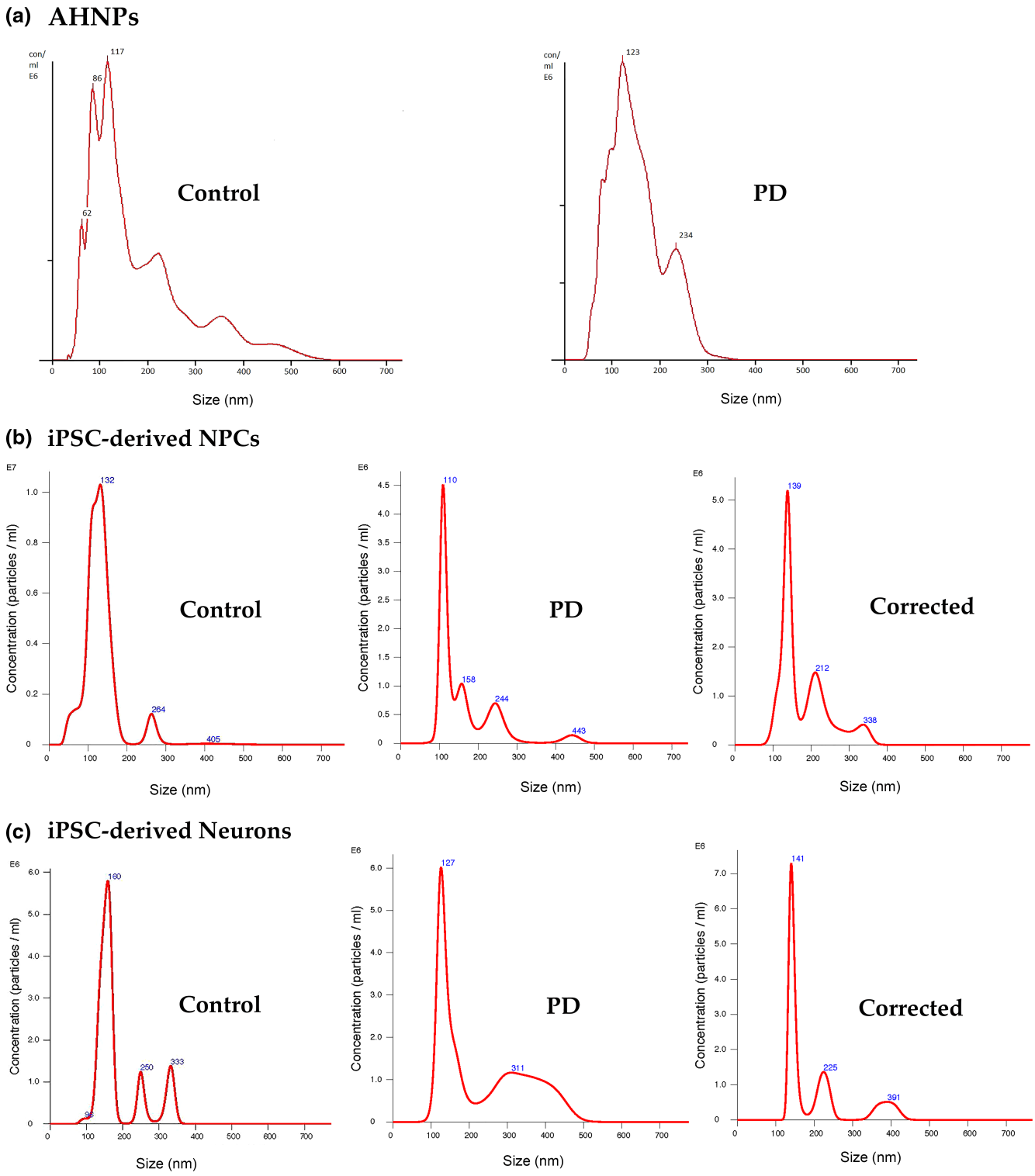

FIGURE 3 Nanoparticle tracking analysis using Nanosight. Vesicles from conditioned media of cultured cells were analyzed for vesicle size and number. (a) Concentration of EMVs was measured in conditioned media from cultured control and Parkinson's (PD) brain-derived adult human neural progenitor cells. (b) Concentration of EMVs was measured in conditioned media from control, LRRK2 mutant (PD), and corrected iPSC-derived neural progenitor cells. (c) Concentration of EMVs was measured in conditioned media from control, LRRK2 mutant (PD), and corrected iPSC-derived dopaminergic neurons [Color figure can be viewed at wileyonlinelibrary.com]

abundant vesicle size (statistical mode). A graphical representation of Nanosight analysis over several passages of neural precursor cells shows that control NPCs (from PI-18) have more, larger vesicles than two clones of the LRRK2 G2019S mutation (heterozygous, PI-1.13, and Coriell ND40018). NPCs from the G/S corrected line have vesicles in a similar size to the controls at passage 16.

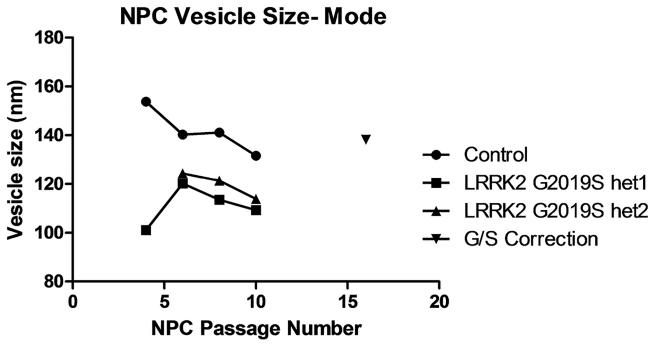

FIGURE 4 LRRK2 G2019S mutations alter the most abundant vesicle size. Vesicle sizes remain fairly constant across NPC passages of the two LRRK2 cases, whereas the highest passage corrected line approaches the highest passage of the control

3.3 | Gene correction of the LRRK2 G2019S mutation results in neuronal EMV cargo gene expression similar to controls

Exosomes have been shown to package important genomic and proteomic information, including DNA, RNA, protein, lipids, and miRNA. To examine gene expression by the EMVs shed from the different cell lines, RNA was isolated from EMVs released from iPSC-derived dopaminergic neurons using the exoRNeasy kit. We have previously reported that vesicles isolated using the columns in this kit express exosome markers (Enderle et al., 2015). Relative gene expression from extracted RNA was analyzed using a TaqMan OpenArray Human Stem Cell Plate. Analysis of gene expression shows alterations of many genes (see Supporting Information for a list of these genes) in the G2019S mutant line as compared with the control and corrected cell lines. Comparison of the G/S corrected line to the control line, however, reveals few alterations in gene expression, suggesting that the exosomes from the corrected line have similar gene expression as the control line (Figure 5a). For a closer examination of the data, we generated a heat map showing gene expression of several genes known previously to be involved in neurodegenerative disorders and compared gene expression of EMVs shed from each cell line (Figure 5b) (Jayapalan, Subramanian, & Natarajan, 2016). These genes were further plotted in a histogram (Figure 5c) that further revealed the degree of gene correction of a select number of stem cell and chronic tissue inflammation-associated markers from these culture-derived neural exosomes. These data further suggest that gene expression changes in exosomes from LRRK2 G2019S mutant dopaminergic neurons are specific to the point mutation of the gene.

4 | DISCUSSION

The present study has demonstrated the ability to generate and molecularly profile EMVs from both idiopathic and LRRK2 gene-identified neural cells. Through the reprogramming and subsequent in vitro differentiation of patient-obtained cells, we were able to make dopaminergic neurons that mimic cells found in patient brain. iPSC-derived PD neural cells were compared, for the first time, with an indigenous population of adult human brain neural progenitor cells, AHNPs, isolated and expanded from postmortem PD and control brain specimens that we have characterized previously (Walton et al., 2006; Wang et al., 2012). By performing these studies, we were ultimately able to collect and characterize EMVs from these cells, control, LRRK2 mutant, and corrected LRRK2 neurons. These analyses revealed marked changes in gene expression of commonly associated with neurodegenerative diseases, which appeared to return to control levels in LRRK2 corrected neuronal EMVs.

Our discovery of the AHNP has allowed us to utilize neural stem/progenitor cells isolated directly from patients and give us a tool to study cells from the brain ex vivo. However, these AHNPs were from patients with idiopathic PD, meaning an unknown origin of PD development. The ability to reprogram and differentiate skin fibroblasts offers a tool to study cells from a patient with PD with a known genetic mutation, as well as control patients. In these studies, we used iPSCs created from skin fibroblasts from a patient with a LRRK2 mutation (Nguyen et al., 2011; Sanders et al., 2014). From these iPSCs, we generated NPCs that were further differentiated into dopaminergic neurons. This yielded NPCs derived from an adult human with a known genetic background from which EMVs could be collected and analyzed. A limitation of the current study is that we only aimed to establish that these iPSC-derived cells exhibited characteristics of bona fide human neural cells in order to perform the genetic and molecular analyses of their released EMVs. Since we did not study and establish the potential dopaminergic, e.g., TH expression of transplanted cells as we determined in vitro here, largely because under the conditions and post-transplantation survival times utilized here DCX and other neuronal markers revealed an immature phenotype of these cells, future in vivo studies including further characterization of xenografted PD-at risk cells should include such deeper analyses to help confirm and extend the in vitro EMV molecular characterization findings presented here.

Our aim of this study was to relate LRRK2 mutations and a potential extracellular synucleinopathy to EMVs, employing for the first-time iPSC-derived dopamine neuronal progenitor cells from a patient with a LRRK2 G2019S mutation. In this study, we found that EMVs are released from iPSC-derived neural cells with an LRRK2 G2019S mutation and that LRRK2 G2019S mutant EMVs were found to be different from healthy control EMVs. Such findings have the potential to contribute to the identification of new and more sensitive biomarkers for PD, at the same time implicating EMVs as a future diagnostic. It has been previously reported that there are elevated levels of extracellular α-syn in iPSC-derived dopaminergic neurons, putatively involving ER stress and altered autophagic function (Fernandes et al., 2016). Previous work using the LRRK2 iPSCs studied here revealed mitochondrial DNA damage that was reversed using the zinc-finger nuclease gene editing approach (Sanders et al., 2014). Mutations in the LRRK2 endocytotic pathway have been discussed in light of altered neuronal synaptic vesicle endocytosis and exocytosis, including increases in the number of multivesicular bodies that impacts EMV release and action as described here (Gupta & Pulliam, 2014). These same authors propose that a buildup of these "mutant" exosomes that are potentially enriched in toxic, disease-associated proteins including alpha-synuclein could facilitate infectious

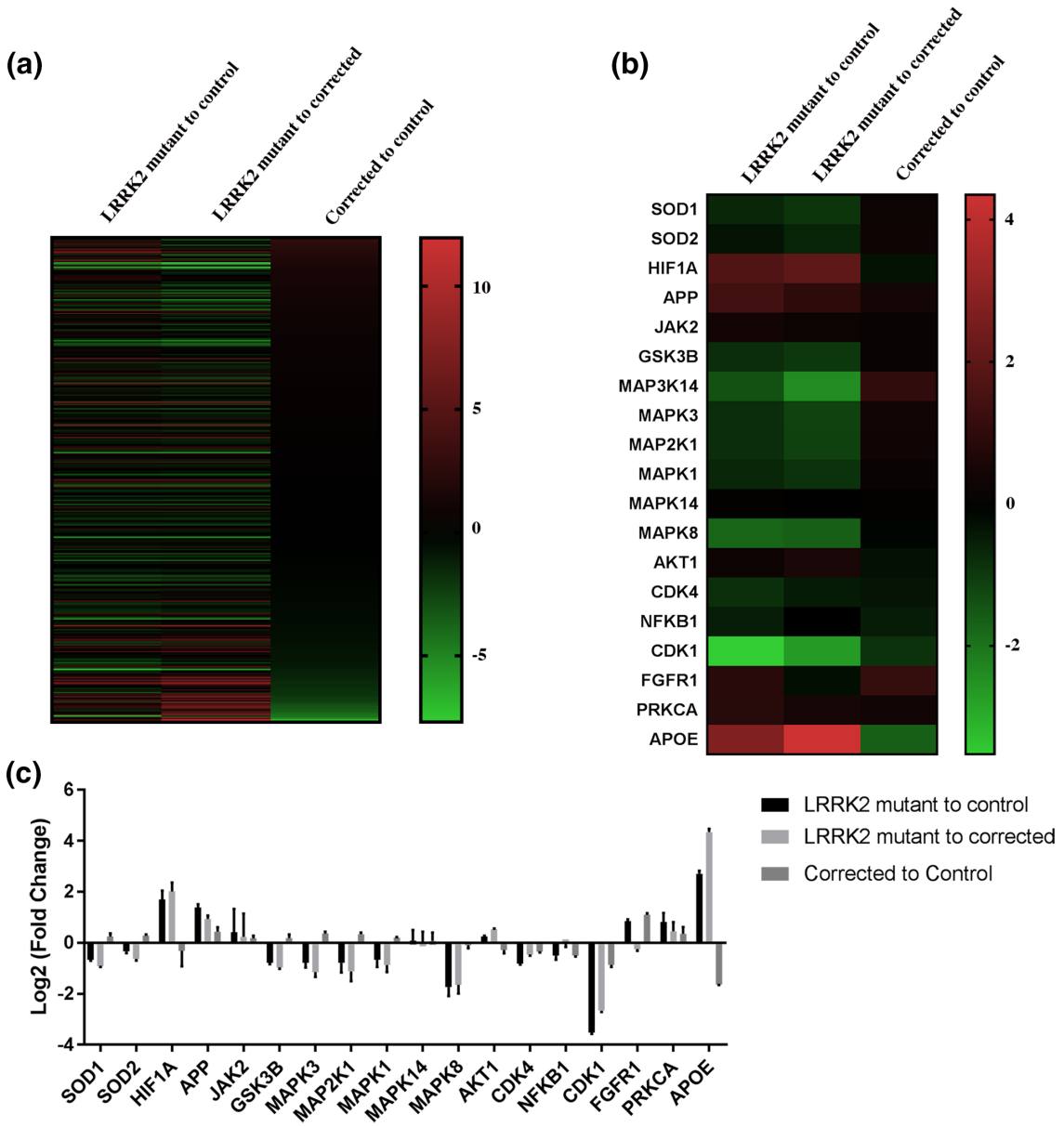

FIGURE 5 Relative gene expression in EMVs isolated from iPSC-derived dopaminergic neurons. Heat map showing relative gene expression of human embryonic stem cell-related genes from EMVs isolated from iPSC-derived dopaminergic neurons. Data are shown as a log2-fold change in gene expression as compared with the other cell line for that column. The red color indicates an increase in the expression of a gene, black indicates no change in gene expression, and green indicates a decrease in gene expression. Relative gene expression was compared between LRRK2 G2019S mutant (1.13) to control (1815), LRRK2 G2019S mutant (1.13) to the zinc-finger corrected line (1.7), and the zinc-finger corrected (1.7) line to control (1815). Samples were loaded in duplicate. (a) Relative gene expression changes of all 355 measureable genes using the TaqMan OpenArray human stem cell plate. (b) Of the 355 genes analyzed in (a), relative gene expression is shown for genes known to be involved in neurodegenerative disorders. As for quality control of the RNA, our readout of the assay is qPCR, so we use that as a readout for RNA quality. The samples were of good quality and had robust detection of the target genes (for example maximum dropout of only 1 out of the 22 control assays). (c) Relative gene expression in exosomes isolated from iPSC-derived dopaminergic neurons as mapped in (a) and (b) [Color figure can be viewed at wileyonlinelibrary.com]

transmission and spread of disease that accounts for progression (Candelario & Steindler, 2014) where lysosomal dysfunction associated with PD helps to mediate the increase in exosomal alpha-synuclein transmission (Alvarez-Erviti et al., 2011). Altered LRRK2 exosomal release is regulated by 14–3-3 (Fraser et al., 2013) and itself has been shown to be present, elevated and informative as to predicting parkinsonian phenotype and potentially disease status in general in PD urinary exosomes (Fraser, Moehle, et al., 2016; Fraser, Rawlins, et al., 2016). Functionally, exosomal alpha-synuclein isolated from cerebrospinal fluid has been shown to induce oligomerization of this protein (Stuendl et al., 2016).

Even though we have compared primary cell lines from several idiopathic along with gene-identified cases, including control, a heterozygote sibling and gene corrected LRRK2 iPSC lines, more such

cases should be interrogated in order to substantiate the molecular profiling findings. This is especially relevant with regard to cautions issued on "small but significant…inter- and intrapatient variations in iPSC cell-based disease modeling" (Sgodda & Cantz, 2013). Certainly, it is difficult to define how many cases or lines from a single case are needed in order to avoid an underpowered study. Human stem cell and especially reprogrammed stem cell disease modeling studies are still establishing such parameters, but it is noteworthy that numerous studies beyond the current one build on the analysis of this LRRK2 G2019S mutation originally described by one of the authors and focusing on an exemplary gene identified case (Nguyen et al., 2011); in many ways, this case and these iPSC lines are still exemplary of this gene-identified PD phenotype and still worthy of study in comparison with a sibling control and gene corrected lines, in addition to idiopathic PD cases (the AHNP studies, as originally described in Wang et al., 2012). Furthermore, numerous iPSC studies with extreme clinical relevance have relied on the same or even smaller sample sizes, be it either chromosomal aberrations including duplications as in certain psychiatric disorders as from a single 5q11.2-q13.1 duplication syndrome patient (Arioka, Kushima, Mori, & Ozaki, 2018) or chromosomal rearrangements involved in reproduction (Mouka et al., 2017), or analysis of iPSC-derived retinal cells from one patient with macular degeneration (Mandai et al., 2017), these studies do provide significant and important cell and molecular information toward establishing the molecular signatures of different human stem cell populations in spite of inherent cross-patient omics variability that nonetheless exhibit much less disparity between biological replicates from the same case. The analysis of exosomes from the current cases adheres to guidelines established by one of the authors for satisfying minimal information requirements for studies of extracellular vesicles and their distinctive and patient−/disease-specific RNA, DNA, and protein cargoes (Thery et al., 2018). Heterogeneity issues in the iPSC field of study are in many ways reminiscent of such in the study of human stem cells as well, where we showed distinctive intrapatient variability in the cell and molecular phenotype of clones derived from a single neurogenic subventricular zone specimen (Suslov, Kukekov, Ignatova, & Steindler, 2002). Even with significant caveats of such *n* of 1 or single patient studies, such analyses provide exemplary findings and characterizations that are most often replicated in large case number studies; at the least eventually leading to the stratification of patients and associated genetic, molecular and cellular biomarkers that can define heterogeneous disease risk and progression phenotypes.

As we have shown in this study by comparing exosomal cargoes of control and gene-corrected EMVs, there is precedence for cellular release of subpopulations of exosomes with distinct molecular properties (Willms et al., 2016). We measured the gene expression of stem-cell related genes that are used to characterize human embryonic stem cells. Comparison of EMVs from LRRK2 mutant iPSC-derived dopaminergic neurons to both control and gene-corrected iPSC-derived dopaminergic neurons, we found significant gene expression changes that were returned to control levels in the gene-corrected EMVs. Of the genes analyzed, we identified several that have been shown to be involved in neurodegenerative diseases, including expression patterns associated with neuroinflammation and immune function that we know are involved in PD (Cook et al., 2017; Lee, Chung, McAlpine, & Tansey, 2011). We document here EMV cargo gene correction of a few genes that are relevant to both stem cell behavior and neurodegeneration, including SOD1, SOD2, HIF1a, APP, JAK2, GSK3B, and several other protein kinases (Jayapalan et al., 2016). Previous studies have shown a significant change in gene expression resulting from this LRRK2 mutation related to inflammation as seen in both prodromal and clinical PD in general (Brockmann et al., 2016). A study by Walker and colleagues has provided a detailed and extensive list of inflammation- and trophic molecule-associated expressions within the substantia nigra and striatum in PD versus Lewy Body Disease and controls that can be a framework for future studies of PD-representative EMVs that should highlight the importance of particular inflammatory networks for better diagnosis and treatment of different neurodegenerative diseases with often overlapping phenotypes (Walker et al., 2015). In that study, the authors report that, for example, IL-15, IL-6sR, ErbB3, IL-2, and PF4 show significant sensitivity toward discriminating these different diseases. A variety of microRNAs also have been associated with pathological EMV release in PD (Brites & Fernandes, 2015; Gui et al., 2015). Dysregulated miRNAs, exosomes, ectosomes, and microglia have been proposed to be associated with the high inflammatory tone associated with disease propagation in PD and other neurodegenerative diseases (Brites & Fernandes, 2015). Brites and Fernandes (2015) describe the brain's innate immune cells, microglia, associated with exosomal cargoes containing for example IL-6, IL-1b, TNF-alpha, NF-Kb, MAPKs, and JNK1/1 associated with reactive microglia following LPS activation (Brites & Fernandes, 2015). In addition to microglia circumscribing amyloid plaques in the Alzheimer's brain, proteins associated with EMV membranes including Alix and flotillin-1 also surround plaques (for review, see Gupta & Pulliam (2014)). That, plus a growing connection between immune system malfunction and autoimmunity in PD (Witoelar et al., 2017) and the presence of LRRK2 in the gut (Maekawa et al., 2017), as well as and a putative role in Crohn's disease (Fujioka et al., 2017) in addition to PD (Shannon et al., 2012), together suggest that further work is needed on the infectious nature of PD and how its potential propagation is helped to be mediated by EMVs carrying abnormal proteins and nucleic acids.

ACKNOWLEDGMENTS

This research was funded by the Michael J. Fox Foundation for Parkinson's Research. D. A. S. and T. Z. are supported by USDA/ARS grant 1950-51000-081-00D. This study used samples from the NINDS Human Genetics Resource Center DNA and Cell Line Repository (https://catalog.coriell.org/1/ninds), as well as associated clinical data. NINDS Repository sample numbers corresponding to the samples used are: ND41865, ND40018, and ND40019. The GFP lenti-viral vector was a kind gift from Dr. Lung-Ji Chang, University of Florida. The authors thank Sohyun Lee, Scott Stratman, and Simeon Walton for technical assistance, Dr. Florian Siebzehnrubl for guidance, and members of Dr. Xandra Breakfield's Laboratory for helpful discussion.

CONFLICT OF INTEREST

Dr. Johan Skog conducted his work as a full-time employee at Exosome Diagnostics Inc. Waltham, MA. The funders provided support in the form of salaries for authors (K.M.C., D.A.S., and T.Z.), but did not have any additional role in the study design, data collection and analysis, decision to publish, or preparation of the manuscript.

AUTHOR CONTRIBUTIONS

K.M.C. and D.A.S. designed the study and the experiments. All the authors helped with the execution and interpretation of the experiments. B.S. from Stanford provided iPS cells, and B.S. (Germany) also provided AHNP cells.

DATA AVAILABILITY STATEMENT

Data available on request from the authors.

ORCID

Kate M. Candelario https://orcid.org/0000-0003-2290-2657
Dennis A. Steindler https://orcid.org/0000-0002-9891-8455

REFERENCES

Arioka, Y., Kushima, I., Mori, D., & Ozaki, N. (2018). Three lines of induced pluripotent stem cells derived from a 15q11.2-q13.1 duplication syndrome patient. *Stem Cell Research*, *31*, 240–243. https://doi.org/10.1016/j.scr.2018.08.004

Alvarez-Erviti, L., Seow, Y., Schapira, A. H., Gardiner, C., Sargent, I. L., Wood, M. J., & Cooper, J. M. (2011). Lysosomal dysfunction increases exosome-mediated alpha-synuclein release and transmission. *Neurobiology of Disease*, *42*(3), 360–367. https://doi.org/10.1016/j.nbd.2011.01.029

Braak, H., & Del Tredici, K. (2009). Neuroanatomy and pathology of sporadic Parkinson's disease. *Advances in Anatomy, Embryology, and Cell Biology*, *201*, 1–119.

Brites, D., & Fernandes, A. (2015). Neuroinflammation and depression: Microglia activation, extracellular microvesicles and microRNA dysregulation. *Frontiers in Cellular Neuroscience*, *9*(476), 1–20. https://doi.org/10.3389/fncel.2015.00476

Brockmann, K., Apel, A., Schulte, C., Schneiderhan-Marra, N., Pont-Sunyer, C., Vilas, D., … Maetzler, W. (2016). Inflammatory profile in LRRK2-associated prodromal and clinical PD. *Journal of Neuroinflammation*, *13*(1), 122. https://doi.org/10.1186/s12974-016-0588-5

Burke, R. E., Dauer, W. T., & Vonsattel, J. P. (2008). A critical evaluation of the Braak staging scheme for Parkinson's disease. *Annals of Neurology*, *64*(5), 485–491. https://doi.org/10.1002/ana.21541

Burre, J., Sharma, M., Tsetsenis, T., Buchman, V., Etherton, M. R., & Sudhof, T. C. (2010). Alpha-synuclein promotes SNARE-complex assembly in vivo and in vitro. *Science*, *329*(5999), 1663–1667. https://doi.org/, https://doi.org/10.1126/science.1195227

Cai, X., Janku, F., Zhan, Q., & Fan, J. B. (2015). Accessing genetic information with liquid biopsies. *Trends in Genetics*, *31*(10), 564–575. https://doi.org/10.1016/j.tig.2015.06.001

Candelario, K. M., & Steindler, D. A. (2014). The role of extracellular vesicles in the progression of neurodegenerative disease and cancer. *Trends in Molecular Medicine*, *20*(7), 368–374. https://doi.org/10.1016/j.molmed.2014.04.003

Cook, D. A., Kannarkat, G. T., Cintron, A. F., Butkovich, L. M., Fraser, K. B., Chang, J., … Tansey, M. G. (2017). LRRK2 levels in immune cells are increased in Parkinson's disease. *NPJ Parkinsons Disease*, *3*, 11. https://doi.org/10.1038/s41531-017-0010-8

Cookson, M. R., & Bandmann, O. (2010). Parkinson's disease: Insights from pathways. *Human Molecular Genetics*, *19*(R1), R21–R27. https://doi.org/10.1093/hmg/ddq167

Eitan, E., Suire, C., Zhang, S., & Mattson, M. P. (2016). Impact of lysosome status on extracellular vesicle content and release. *Ageing Research Reviews*, *32*, 65–74. https://doi.org/10.1016/j.arr.2016.05.001

Enderle, D., Spiel, A., Coticchia, C. M., Berghoff, E., Mueller, R., Schlumpberger, M., … Noerholm, M. (2015). Characterization of RNA from exosomes and other extracellular vesicles isolated by a novel spin column-based method. *PLoS One*, *10*(8), e0136133. https://doi.org/10.1371/journal.pone.0136133

Fernandes, H. J., Hartfield, E. M., Christian, H. C., Emmanoulidou, E., Zheng, Y., Booth, H., … Wade-Martins, R. (2016). ER stress and autophagic perturbations lead to elevated extracellular alpha-synuclein in GBA-N370S Parkinson's iPSC-derived dopamine neurons. *Stem Cell Reports*, *6*(3), 342–356. https://doi.org/10.1016/j.stemcr.2016.01.013

Fraser, K. B., Moehle, M. S., Alcalay, R. N., West, A. B., & Consortium, L. C. (2016). Urinary LRRK2 phosphorylation predicts parkinsonian phenotypes in G2019S LRRK2 carriers. *Neurology*, *86*(11), 994–999. https://doi.org/10.1212/WNL.0000000000002436

Fraser, K. B., Moehle, M. S., Daher, J. P., Webber, P. J., Williams, J. Y., Stewart, C. A., … West, A. B. (2013). LRRK2 secretion in exosomes is regulated by 14-3-3. *Human Molecular Genetics*, *22*(24), 4988–5000. https://doi.org/10.1093/hmg/ddt346

Fraser, K. B., Rawlins, A. B., Clark, R. G., Alcalay, R. N., Standaert, D. G., Liu, N., … West, A. B. (2016). Ser(P)-1292 LRRK2 in urinary exosomes is elevated in idiopathic Parkinson's disease. *Movement Disorders*, *31*(10), 1543–1550. https://doi.org/10.1002/mds.26686

Fujioka, S., Curry, S. E., Kennelly, K. D., Tacik, P., Heckman, M. G., Tsuboi, Y., … Wszolek, Z. K. (2017). Occurrence of Crohn's disease with Parkinson's disease. *Parkinsonism & Related Disorders*, *37*, 116–117. https://doi.org/10.1016/j.parkreldis.2017.01.013

Goetz, A. K., Scheffler, B., Chen, H. X., Wang, S., Suslov, O., Xiang, H., … Steindler, D. A. (2006). Temporally restricted substrate interactions direct fate and specification of neural precursors derived from embryonic stem cells. *Proceedings of the National Academy of Sciences of the United States of America*, *103*(29), 11063–11068. https://doi.org/10.1073/pnas.0510926103

Gui, Y., Liu, H., Zhang, L., Lv, W., & Hu, X. (2015). Altered microRNA profiles in cerebrospinal fluid exosome in Parkinson disease and Alzheimer disease. *Oncotarget*, *6*(35), 37043–37053. https://doi.org/10.18632/oncotarget.6158

Gupta, A., & Pulliam, L. (2014). Exosomes as mediators of neuroinflammation. *Journal of Neuroinflammation*, *11*, 68. https://doi.org/10.1186/1742-2094-11-68

Israel, M. A., Yuan, S. H., Bardy, C., Reyna, S. M., Mu, Y., Herrera, C., … Goldstein, L. S. (2012). Probing sporadic and familial Alzheimer's disease using induced pluripotent stem cells. *Nature*, *482*(7384), 216–220. https://doi.org/10.1038/nature10821

Jang, H., Boltz, D., Sturm-Ramirez, K., Shepherd, K. R., Jiao, Y., Webster, R., & Smeyne, R. J. (2009). Highly pathogenic H5N1 influenza virus can enter the central nervous system and induce neuroinflammation and neurodegeneration. *Proceedings of the National Academy of Sciences of the United States of America*, *106*(33), 14063–14068. https://doi.org/10.1073/pnas.0900096106

Jayapalan, S., Subramanian, D., & Natarajan, J. (2016). Computational identification and analysis of neurodegenerative disease associated protein kinases in hominid genomes. *Genes & Diseases*, *3*(3), 228–237. https://doi.org/10.1016/j.gendis.2016.04.004

Kordower, J. H., Chu, Y., Hauser, R. A., Freeman, T. B., & Olanow, C. W. (2008). Lewy body-like pathology in long-term embryonic nigral transplants in Parkinson's disease. *Nature Medicine*, *14*(5), 504–506. https://doi.org/10.1038/nm1747

Lee, J. K., Chung, J., McAlpine, F. E., & Tansey, M. G. (2011). Regulator of G-protein signaling-10 negatively regulates NF-kappaB in microglia and neuroprotects dopaminergic neurons in hemiparkinsonian rats. *The Journal of Neuroscience*, *31*(33), 11879–11888. https://doi.org/10.1523/JNEUROSCI.1002-11.2011

Loov, C., Scherzer, C. R., Hyman, B. T., Breakefield, X. O., & Ingelsson, M. (2016). Alpha-synuclein in extracellular vesicles: Functional implications and diagnostic opportunities. *Cellular and Molecular Neurobiology*, *36*(3), 437–448. https://doi.org/10.1007/s10571-015-0317-0

Maekawa, T., Shimayama, H., Tsushima, H., Kawakami, F., Kawashima, R., Kubo, M., & Ichikawa, T. (2017). LRRK2: An emerging new molecule in the enteric neuronal system that quantitatively regulates neuronal peptides and IgA in the gut. *Digestive Diseases and Sciences*, *62*(4), 903–912. https://doi.org/10.1007/s10620-017-4476-3

Mak, S. K., Huang, Y. A., Iranmanesh, S., Vangipuram, M., Sundararajan, R., Nguyen, L., … Schule, B. (2012). Small molecules greatly improve conversion of human-induced pluripotent stem cells to the neuronal lineage. *Stem Cells International*, *2012*, 1–12. https://doi.org/10.1155/2012/140427

Mandai, M., Watanabe, A., Kurimoto, Y., Hirami, Y., Morinaga, C., Daimon, T., et al. (2017). Autologous induced stem-cell-derived retinal cells for macular degeneration. *The New England Journal of Medicine*, *376*(11), 1038–1046. https://doi.org/10.1056/NEJMoa1608368

Mouka, A., Izard, V., Tachdjian, G., Brisset, S., Yates, F., Mayeur, A., et al. (2017). Induced pluripotent stem cell generation from a man carrying a complex chromosomal rearrangement as a genetic model for infertility studies. *Scientific Reports*, *7*, 39760. https://doi.org/10.1038/srep39760

Nemani, V. M., Lu, W., Berge, V., Nakamura, K., Onoa, B., Lee, M. K., … Edwards, R. H. (2010). Increased expression of alpha-synuclein reduces neurotransmitter release by inhibiting synaptic vesicle reclustering after endocytosis. *Neuron*, *65*(1), 66–79. https://doi.org/10.1016/j.neuron.2009.12.023

Ngo HM, Zhou Y, Lorenzi H, Wang K, Kim TK, Zhou Y, El Bissati K, Mui E, Fraczek L, Rajagopala SV et al. 2017. Toxoplasma Modulates Signature Pathways of Human Epilepsy, Neurodegeneration & Cancer. Sci Rep 7 (1):11496. https://doi.org/10.1038/s41598-017-10675-6

Nguyen, H. N., Byers, B., Cord, B., Shcheglovitov, A., Byrne, J., Gujar, P., … Pera, R. R. (2011). LRRK2 mutant iPSC-derived DA neurons demonstrate increased susceptibility to oxidative stress. *Cell Stem Cell*, *8*(3), 267–280. https://doi.org/10.1016/j.stem.2011.01.013

Pfeiffer, R. F. (2012). Autonomic dysfunction in Parkinson's disease. *Expert Review of Neurotherapeutics*, *12*(6), 697–706. https://doi.org/10.1586/ern.12.17

Rajendran, L., Bali, J., Barr, M. M., Court, F. A., Kramer-Albers, E. M., Picou, F., … Breakefield, X. O. (2014). Emerging roles of extracellular vesicles in the nervous system. *The Journal of Neuroscience*, *34*(46), 15482–15489. https://doi.org/10.1523/JNEUROSCI.3258-14.2014

Sanders, L. H., Laganiere, J., Cooper, O., Mak, S. K., Vu, B. J., Huang, Y. A., … Schule, B. (2014). LRRK2 mutations cause mitochondrial DNA damage in iPSC-derived neural cells from Parkinson's disease patients: Reversal by gene correction. *Neurobiology of Disease*, *62*, 381–386. https://doi.org/10.1016/j.nbd.2013.10.013

Sgodda, M., & Cantz, T. (2013). Small but significant: Inter- and intrapatient variations in iPS cell-based disease modeling. *Molecular Therapy*, *21*(1), 5–7. https://doi.org/10.1038/mt.2012.273

Shannon, K. M., Keshavarzian, A., Mutlu, E., Dodiya, H. B., Daian, D., Jaglin, J. A., & Kordower, J. H. (2012). Alpha-synuclein in colonic submucosa in early untreated Parkinson's disease. *Movement Disorders*, *27*(6), 709–715. https://doi.org/10.1002/mds.23838

Steindler, D. A., Okun, M. S., & Scheffler, B. (2012). Stem cell pathologies and neurological disease. *Modern Pathology*, *25*(2), 157–162. https://doi.org/10.1038/modpathol.2011.16

Stuendl, A., Kunadt, M., Kruse, N., Bartels, C., Moebius, W., Danzer, K. M., … Schneider, A. (2016). Induction of alpha-synuclein aggregate formation by CSF exosomes from patients with Parkinson's disease and dementia with Lewy bodies. *Brain*, *139*(Pt2), 481–494. https://doi.org/10.1093/brain/awv346

Suslov, O. N., Kukekov, V. G., Ignatova, T. N., & Steindler, D. A. (2002). Neural stem cell heterogeneity demonstrated by molecular phenotyping of clonal neurospheres. *Proceedings of the National Academy of Sciences of the United States of America*, *99*(22), 14506–14511. https://doi.org/10.1073/pnas.212525299

Thery, C., Amigorena, S., Raposo, G., & Clayton, A. (2006). Isolation and characterization of exosomes from cell culture supernatants and biological fluids. *Current Protocols in Cell Biology*, *3*, 22–3.22.29. https://doi.org/10.1002/0471143030.cb0322s30

Thery, C., Witwer, K. W., Aikawa, E., Alcaraz, M. J., Anderson, J. D., Andriantsitohaina, R., et al. (2018). Minimal information for studies of extracellular vesicles 2018 (MISEV2018): A position statement of the International Society for Extracellular Vesicles and update of the MISEV2014 guidelines. *Journal of Extracellular Vesicles*, *7*(1), 1535750. https://doi.org/10.1080/20013078.2018.1535750

Tomlinson, P. R., Zheng, Y., Fischer, R., Heidasch, R., Gardiner, C., Evetts, S., … Tofaris, G. K. (2015). Identification of distinct circulating exosomes in Parkinson's disease. *Annals of Clinical Translational Neurology*, *2*(4), 353–361. https://doi.org/10.1002/acn3.175

Urnov, F. D., Miller, J. C., Lee, Y. L., Beausejour, C. M., Rock, J. M., Augustus, S., … Holmes, M. C. (2005). Highly efficient endogenous human gene correction using designed zinc-finger nucleases. *Nature*, *435*(7042), 646–651. https://doi.org/10.1038/nature03556

Walker, D. G., Lue, L. F., Serrano, G., Adler, C. H., Caviness, J. N., Sue, L. I., & Beach, T. G. (2015). Altered expression patterns of inflammation-associated and trophic molecules in Substantia Nigra and striatum brain samples from Parkinson's disease, incidental Lewy body disease and normal control cases. *Frontiers in Neuroscience*, *9*, 507. https://doi.org/10.3389/fnins.2015.00507

Walton, N. M., Sutter, B. M., Chen, H. X., Chang, L. J., Roper, S. N., Scheffler, B., & Steindler, D. A. (2006). Derivation and large-scale expansion of multipotent astroglial neural progenitors from adult human brain. *Development*, *133*(18), 3671–3681. https://doi.org/10.1242/dev.02541

Wang, S., Okun, M. S., Suslov, O., Zheng, T., McFarland, N. R., Vedam-Mai, V., … Steindler, D. A. (2012). Neurogenic potential of progenitor cells isolated from postmortem human Parkinsonian brains. *Brain Research*, *1464*, 61–72. https://doi.org/10.1016/j.brainres.2012.04.039

Willms, E., Johansson, H. J., Mager, I., Lee, Y., Blomberg, K. E., Sadik, M., … Vader, P. (2016). Cells release subpopulations of exosomes with distinct molecular and biological properties. *Scientific Reports*, *6*, 22519. https://doi.org/10.1038/srep22519

Witoelar, A., Jansen, I. E., Wang, Y., Desikan, R. S., Gibbs, J. R., Blauwendraat, C., … International Parkinson's Disease Genomics Consortium NABEC, United Kingdom Brain Expression Consortium I. (2017). Genome-wide pleiotropy between Parkinson disease and autoimmune diseases. *JAMA Neurology*, *74*(7), 780–792. https://doi.org/10.1001/jamaneurol.2017.0469

Xi, J., Liu, Y., Liu, H., Chen, H., Emborg, M. E., & Zhang, S. C. (2012). Specification of midbrain dopamine neurons from primate pluripotent stem cells. *Stem Cells*, *30*(8), 1655–1663. https://doi.org/10.1002/stem.115

Zhang, S. C., Ge, B., & Duncan, I. D. (2000). Tracing human oligodendroglial development in vitro. *Journal of Neuroscience Research*, *59*(3), 421–429 https://doi.org/10.1002/(SICI)1097-4547(20000201)59:3<421::AID-JNR17>3.0.CO;2-C.

SUPPORTING INFORMATION

Additional supporting information may be found online in the Supporting Information section at the end of this article.

How to cite this article: Candelario KM, Balaj L, Zheng T, et al. Exosome/microvesicle content is altered in leucine-rich repeat kinase 2 mutant induced pluripotent stem cell-derived neural cells. *J Comp Neurol*. 2019;1–13. https://doi.org/10.1002/cne.24819